Dual site-specific chemoenzymatic antibody fragment conjugation using CRISPR-based hybridoma engineering

Gall, C.M. le; Schoot, J.M.S. van der; Ramos-Tomillero, I.; Khalily, M.P.; Dalen, F.J. van; Wijfjes, Z.; ... ; Verdoes, M.

Citation

Note: To cite this publication please use the final published version (if applicable).

Dual Site-Specific Chemoenzymatic Antibody Fragment Conjugation Using CRISPR-Based Hybridoma Engineering

Camille M. Le Gall, Johan M. S. van der Schoot, Iván Ramos-Tomillero, Melek Parlak Khalily, Floris J. van Dalen, Zacharias Wijfjes, Liyan Smeding, Duco van Dalen, Anna Cammarata, Kimberly M. Bonger, Carl G. Figdor, Ferenc A. Scheeren, and Martijn Verdoes*
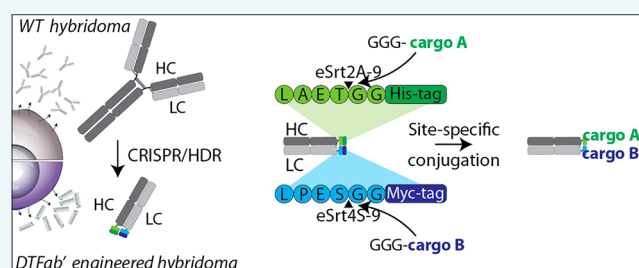
Read Online

ACCESS | Metrics & More | Article Recommendations | Supporting Information

ABSTRACT: Functionalized antibodies and antibody fragments have found applications in the fields of biomedical imaging, theranostics, and antibody−drug conjugates (ADC). In addition, therapeutic and theranostic approaches benefit from the possibility to deliver more than one type of cargo to target cells, further challenging stochastic labeling strategies. Thus, bioconjugation methods to reproducibly obtain defined homogeneous conjugates bearing multiple different cargo molecules, without compromising target affinity, are in demand. Here, we describe a straightforward CRISPR/Cas9-based strategy to rapidly engineer hybridoma cells to secrete Fab′ fragments bearing two distinct site-specific labeling motifs, which can be separately modified by two different sortase A mutants. We show that sequential genetic editing of the heavy chain (HC) and light chain (LC) loci enables the generation of a stable cell line that secretes a dual tagged Fab′ molecule (DTFab′), which can be easily isolated. To demonstrate feasibility, we functionalized the DTFab′ with two distinct cargos in a site-specific manner. This technology platform will be valuable in the development of multimodal imaging agents, theranostics, and next-generation ADCs.

INTRODUCTION

The use of antibody−drug conjugates (ADCs) has emerged as a potent strategy in the treatment of malignancies. As of late 2020, nine FDA-approved ADCs[1−9] are used in the clinic, and several hundred are currently under clinical inestigation.[10] First- and second-generation ADCs are classically produced by conjugation of drug molecules to the side chains of solvent-exposed lysines or interchain cysteines.[11] However, such approaches lead to highly heterogeneous end-products with variable molecular weights, drug coupling sites, and drug-to-antibody ratio (DAR), with the concomitant risk of influencing target binding affinity.[12] Indeed, monoclonal antibodies (mAbs) typically contain more than 60 accessible lysines, whereas the drug-to-antibody ratio (DAR) should remain low enough (3−4) to prevent aggregation.[13,14] Third-generation ADCs aim to address these challenges by using site-specific conjugation methods.[11,12] As opposed to random coupling, site-specific modification enables strict control over payload conjugation to generate a homogeneous product.

Antigen-binding fragments (Fab′) are molecules derived from mAbs.[15] Their heavy chain (HC) is truncated to solely contain the variable domain VH and the constant domain CH1, enabling association with the light chain (LC), but lacks the CH2 and CH3 domains that dimerize to generate the Fc domain. While these Fab′ retain binding ability to their target, they do not exhibit Fc-mediated immune effector functions such as recruitment of effector cells, or fixation of complement.[16] Moreover, they have a shorter half-life in circulation,[17,18] and are more efficient at penetrating dense tissues in which conventional mAbs are excluded.[17,19] However, the probability of modifying the binding region of a Fab′ using classical stochastic labeling is higher than on full-size mAbs, due to the smaller size and reduced number of reaction sites.[20] Thus, Fab′ fragments represent attractive proof-of-concept candidates for third-generation ADCs, as well as for imaging and thera(g)nostic[21] applications.

Functionalization of antibody fragments with distinct payloads is an attractive strategy in for several applications. While combination therapies are gaining more attention in chemotherapeutic treatments, classical ADCs target only one drug to cancer cells. Similarly, multimodal imaging enables the visualization of targets of interest in different scales, from whole body imaging with radioisotopes down to the histological level with fluorescent tracer molecules. These applications would benefit from the development of a flexible
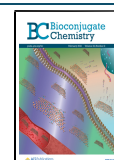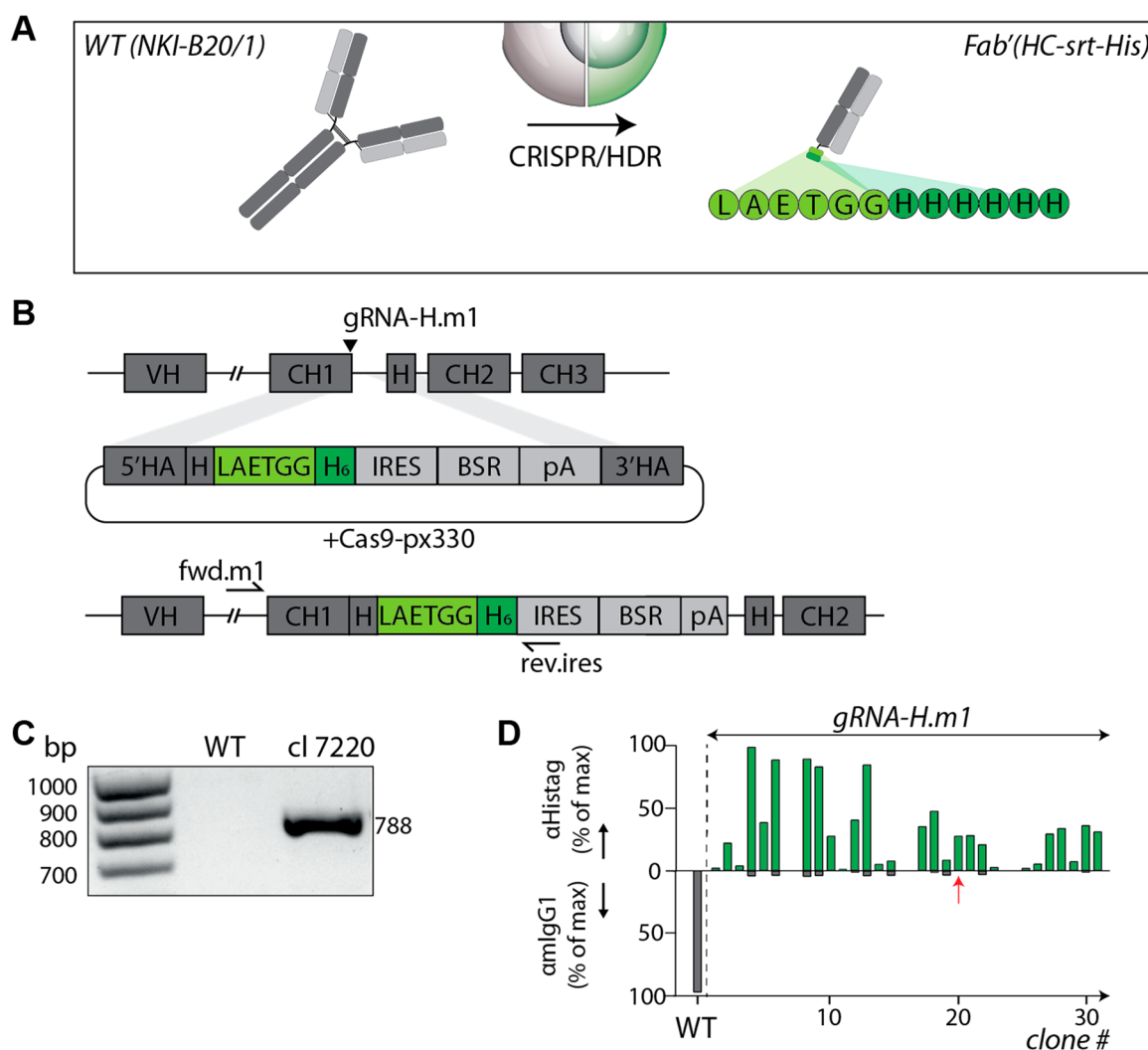
Figure 1. Generation of Fab′ fragment-secreting cell lines from parental hybridoma NKI-B20/1. A,B. General strategy for CRISPR/Cas9 editing. gRNA-H.m1 cuts in the CH1 domain to introduce the first five residues of the hinge region followed by a GGGGS semiflexible linker, a LAETGG sortag motif, and a polyHis-tag (HHHHHH). C. Genomic PCR performed using fwd.m1 and rev.ires primers on DNA isolated from the bulk population after blasticidin selection shows that resistant cells have integrated the inset. D. Mean fluorescence intensity (MFI) of anti-His-tag and anti-mIgG1 on BJAB cells following incubation with antibody-containing supernatants collected from single cell clones shows that most clones have been successfully edited. The red arrow indicates the clone selected for Fab′ production and subsequent genome editing.

plug-and-play antibody fragment engineering platform for dual site-specific labeling. Most site-specific conjugation strategies make use of a short peptide tag (e.g., a sortase A recognition motif[22]) or engineered residues[11,23] to introduce cargos. Thus, they only permit functionalization with multiple distinct payloads through the synthesis of orthogonal multivalent linker systems or multifunctional conjugates, with concomitant synthetic and potential solubility issues. Here, we report a widely applicable strategy to introduce two orthogonal site-selective labeling tags on a Fab′ fragment by capitalizing on our recently reported Clustered Regularly Interspaced Short Palindromic Repeats/Homology Directed Repair (CRISPR/ HDR) hybridoma genomic engineering approach.[24] In this work, we expand the genomic engineering toolbox to enable modification of the HC and LC loci of the mouse IgG1 (mIgG1) hybridoma, available for a plethora of targets. With this, dual-tagged Fab′ (DTFab′) are generated equipped with two distinct sortase A recognition motifs (sortags) on the HC and LC, each orthogonally recognized by a specific variant of the "evolved sortase A" (eSrtA) enzyme (eSrt2A-9 or eSrt4S-

9).[25] These enzymes enable the ligation of virtually any payload bearing a synthetically easily accessible N-terminal polyglycine motif onto the target protein. To demonstrate feasibility, the DTFab′ were sequentially functionalized with two distinct cargos in a site-specific manner, and thoroughly characterized. We expect that this technology platform will be a valuable asset in the development of Fab′ conjugates for imaging, theranostics, and next-generation ADC applications.

■ RESULTS

Generation of a Genetically Engineered Cell Line Secreting Fab′ Fragments. To produce Fab′ fragments suitable for dual site-specific labeling, we sought to alter the immunoglobulin domain within the genome of an anti-hCD20-producing hybridoma cell line, which expresses a mAb of the mIgG1 isotype with a κ LC (Cκ). We hypothesized this could be achieved by adapting our recently developed CRISPR/ HDR approach,[24] in which we genetically engineered the rat IgG2a IgH locus, for modification of the murine IgH and IgK loci. We started with the genetic modification of the HC
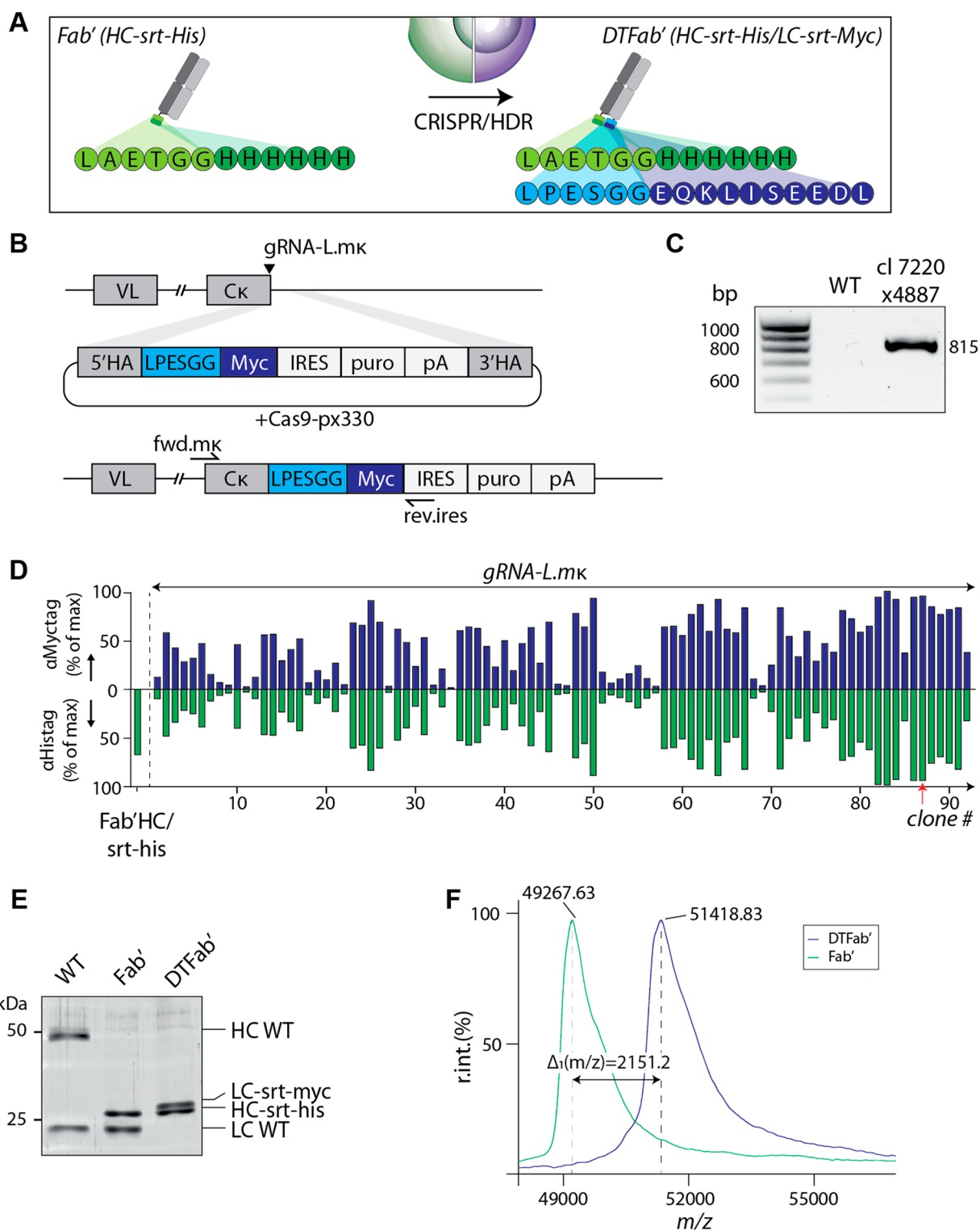
Figure 2. Generation of DTFab′ fragment-secreting cell lines from Fab′ modified hybridoma. A,B. General strategy for CRISPR/Cas9 editing. gRNA-L.mκ cuts in the κ light chain to introduce a GGGGS semiflexible linker, a LPESGG sortag motif, and a Myc-tag (EQKLISEEDL). C. Genomic PCR performed on the bulk population after puromycin selection shows that resistant cells have integrated the inset. D. Mean fluorescence intensity (MFI) of His-tag and anti-Myc-tag on BJAB cells following incubation with antibody-containing supernatants collected from single cell shows near perfect overlap of signals coming from the heavy and light chains for each clone, attesting for a high efficacy of the selection strategy. The red arrow indicates the clone selected for DTFab′ production. E. SDS-PAGE visualization of WT, Fab′, and DTFab′ proteins. F. MALDI-TOF analysis of Fab′ and DTFab′ shows engineering of the LC leads to expected increase of molecular weight, $\Delta_1 = 2151.2$ Da, expected 2059.2 Da.

(Figure 1A and B). To this end, we selected a guide RNA (gRNA-H.m1) that directs the Cas9 protein to the CH1 region of the mIgG1 IgH locus.[26] The HDR template consists of ~600 bp 5′ and 3′ homology arms (HA) flanking the intended
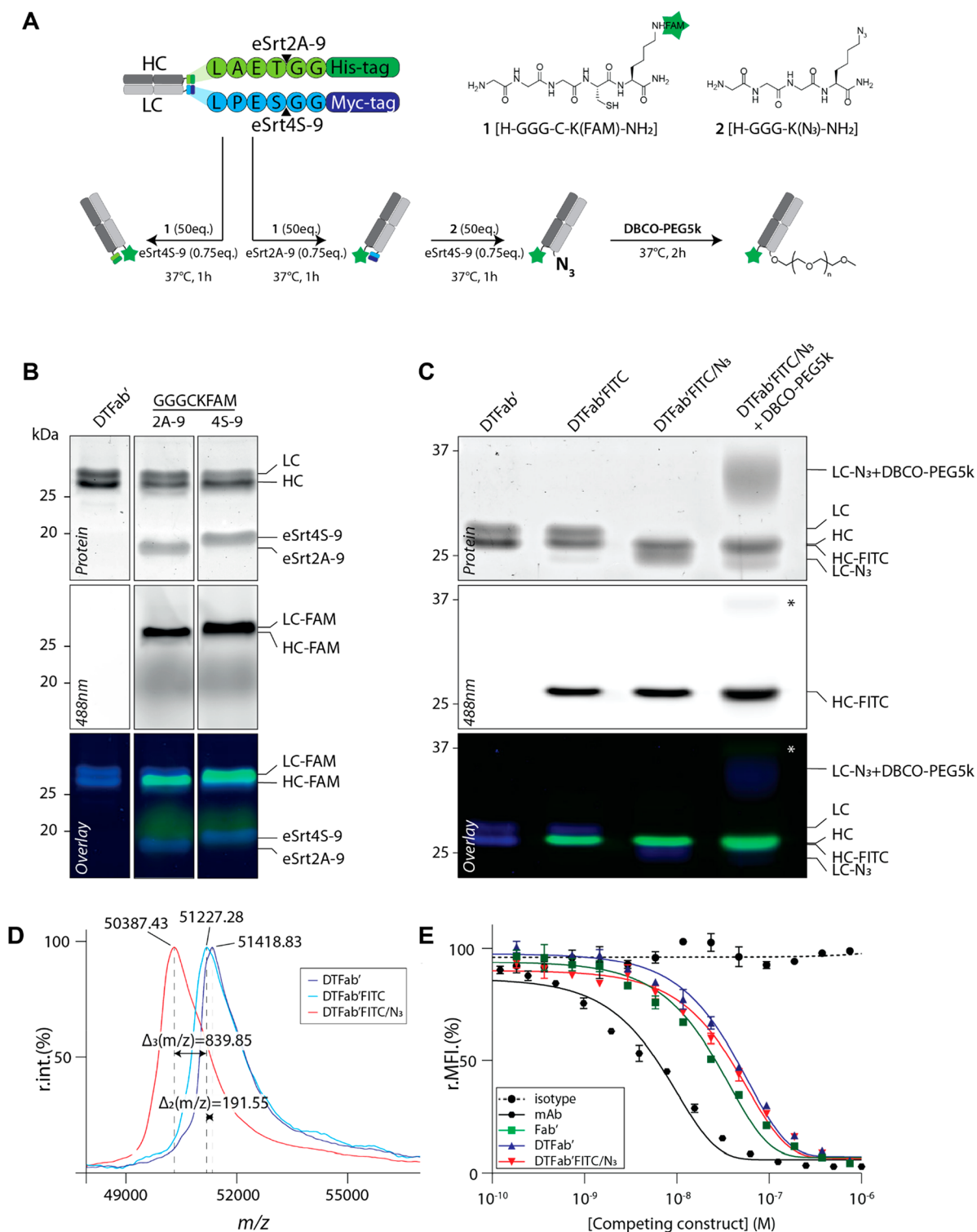
Figure 3. Efficient dual site-specific labeling of DTFab′ onto both HC and LC. A. General strategy, peptides, and conditions used for labeling. Sortase reactions were performed with 50 mol equiv of nucleophile, and 0.75 mol equiv of eSrt4S-9. B. SDS PAGE and fluorescence (488 nm) analysis of sortagging reactions performed separately on the HC (eSrt2A-9) or LC (eSrt4S-9) confirms specificity of the enzymes for their respective cleavage sites. C. SDS PAGE analysis of DTFab′ modified with H-GGG-C-K(FITC)-NH$_2$ on the HC, and H-GGG-K(N$_3$)-NH$_2$ on the LC confirms introduction of two distinct cargos site-specifically onto the engineered Fab′. *: side product in the PEGylation reaction mix: excess of DBCO-PEG reacting with the Cys residue present on peptide **1**. D. MALDI-TOF analysis of DTFab′, DTFab′FITC, and DTFab′FITC/ N$_3$ shows that proteins undergo the expected change in molecular weight during chemoenzymatic ligation (Δ_2 = 191.55 Da, expected 249.21 Da; Δ_3 = 839.85 Da, expected 975.06 Da). E. Antigen binding competition assay of each engineered protein against mAb-AF647 reveals that proteins do not lose binding affinity to their target following CRISPR/Cas9 editing and sequential dual site-specific labeling.

modification site in the hinge region of the HC. It was designed to insert a modified hinge sequence, a GGGGS

linker, the LAETGG tag for chemoenzymatic modification with eSrt2A-9, the hexahistidine-tag (His-tag), and a stop

codon. Additionally, the HDR template contained elements to confer blasticidin resistance upon genomic integration (Table S1). The parental cell line anti-CD20 WT was transfected with the gRNA-H.m1 and HDR template, and subjected to blasticidin selection pressure. Following antibiotic selection, we isolated DNA from the bulk population to confirm the inset integration in resistant cells by PCR. Using a primer that hybridizes directly upstream of the 5′HA, and one specific for the insert (IRES) (Figure 1B), we could detect a unique band at the expected height of 788 bp (Figure 1C), attesting for successful insertion of the HDR template into the targeted locus.

We performed limiting dilution to generate monoclonal cell lines, and after 14 days of culture, we harvested the supernatant of single cell clones, and used it to stain hCD20-expressing BJAB cells (a human Burkitt lymphoma B cell line). To assess genetic engineering, we determined whether the clones were secreting wild-type mAbs or His-tagged Fab′ fragments using secondary antibodies against mIgG1 and His-tag. Supernatant of over 60% of single cell colonies that grew out after antibiotic selection were positive for the His-tag, and negative for mIgG1 signal (Figure 1D), indicating that these edited monoclonal cell lines did not secrete the WT mAb anymore, but instead produced a His-tagged Fab′ fragment. We selected a high-producing monoclonal cell line based on His-tag signal intensity, cell growth rate, and strictly negative mIgG1 signal to eliminate potential contamination with WT cell line (clone 7220, Fab′(HC-srt-his)), and expanded it to pursue the second step of genome editing by genetically modifying the LC to obtain a DTFab′-producing cell line.

Generation of a Genetically Engineered Cell Line Secreting DTFab′ Fragments.
To edit the LC, we designed an HDR template consisting of ~600 bp 5′ and 3′ HA flanking the C-terminus of the κ LC (Cκ), and in-frame inserted an LPESGG sortag for chemoenzymatic modification with eSrt4S-9, and a C-terminal c-Myc epitope tag (Myc-tag, EQKLISE-EDL) for screening purposes (Table S2).

We additionally inserted a puromycin resistance gene (Figure 2B). We selected a guide RNA (gRNA-L.mκ) directing Cas9 to the C-terminus of the LC, and transfected the anti-CD20 Fab′(HC-srt-his)-secreting hybridoma. After puromycin selection, we collected resistant cells, and genomic PCR confirmed insert integration in the Cκ region in this bulk population (Figure 2C). Monoclonal cell lines were obtained by limiting dilution, after which we proceeded with flow cytometry screening, using the monoclonal supernatants to stain hCD20-expressing BJAB cells and to analyze His-tag and Myc-tag signals. Only dual-tagged Fab′ will be equipped with both the His-tag and Myc-tag. Interestingly, most cell lines secreted high levels of Fab′ fragments harboring both His-tag and Myc-tag, while others had overall low production levels (Figure 2D). Importantly, none of the monoclonal cell lines were producing antibody fragments displaying only a His-tag, indicating the robustness of our strategy. A monoclonal cell line (clone7220 × 4887, DTFab′ (LC-srt-Myc)) was selected based on DTFab′ expression level, and expanded for further characterization.

Engineered Antibodies Are Functionalized Site-Specifically and Orthogonally.
Having the parental hybridoma and the two engineered daughter cell lines in hand (WT, Fab′(HC-srt-his) and DTFab′ (HC-srt-his, LC-srt-Myc), respectively), we cultured the cells for antibody production, and purified products from the supernatants. Subsequently, we

analyzed the products by sodium dodecyl sulfate polyacrylamide gel electrophoresis (SDS-PAGE), which confirmed that genomic engineering of the HC resulted in an expected shift from 50 kDa for the WT HC to approximately 25 kDa for the Fab′(HC-srt-his).

Genetic editing of the Igκ locus resulted in an increase of the molecular weight of the LC, in line with the insertion of the LPESGG motif and Myc-tag, as seen by SDS-PAGE and matrix assisted laser desorption ionization-time-of-flight (MALDI-TOF) analysis (Figures 2E,F and S2A). We then proceeded to confirm the orthogonality of the two sortags. The functionality and specificity of the two different sortags were examined by incubating the DTFab′ with either eSrt2A-9 or eSrt4S-9, and an excess of 6-carboxyfluorescein (FAM)-containing substrate peptide 1 (H-GGG-C-K(FAM)-NH$_2$) (Figure 3A). The resulting products were analyzed by fluorescent SDS-PAGE (Figures 3B and S1A). A fluorescent (488 nm (FAM)) protein band was detected, which overlapped with the HC when DTFab′ was reacted in the presence of eSrt2A-9, and conversely, the LC was fluorescently labeled when in the presence of eSrt4S-9. This confirms that the sortag motifs are functional, and that both HC and LC could be functionalized orthogonally with the respective sortase mutants without detectable cross-reactivity.

Dual Site-Specific Labeling of DTFab′ Does Not Hamper Its Binding Affinity.
As a proof-of-concept of dual site-specific modification, we proceeded to sequential sortagging to introduce two different payloads on the DTFab′ (Figure 3A). We first incubated DTFab′ with eSrt2A-9 and an excess of fluorescent peptide 1 (H-GGG-C-K(FITC)-NH$_2$), followed by protein purification (near-quantitative conversion, isolated yield slightly above 60%). The second functionality was introduced by incubation with eSrtA4S-9 and an excess of the azide-functionalized peptide 2 (H-GGG-K(N$_3$)-NH$_2$) and subsequent protein purification (near-quantitative conversion, isolated yield slightly above 50%). All antibody fragments were analyzed by (fluorescent) SDS-PAGE (Figure 3C) and MALDI-TOF (Figures 3D and S2B). As observed by SDS-PAGE analysis, the FITC signal overlaps only with the HC, while ligation of the azido peptide onto the LC leads to a complete shift to a product with a reduced molecular weight, attesting for site-specific incorporation of the cargo. In addition, strain-promoted alkyne−azide cycloaddition (SPAAC) of the dual functionalized Fab′ with an excess of PEG5k-DBCO leads to a selective increase in the size of the LC, showing the functionality of the azide for further diversification of the antibody fragment. MALDI-TOF analysis of the products before and after site-specific modification of the HC and LC confirmed mass changes corresponding to the respective transformations. Finally, to confirm that genome editing and dual site-specific payload conjugation did not affect antigen binding, we performed a competitive antigen binding assay against the AF647-labeled parental antibody on BJAB cells. Analysis of the AF647 signal indicates that all constructs compete with the parental antibody for CD20 binding (Figures 3E and S3B). Importantly, while genetic alteration from a mAb to a Fab′ fragment leads to an expected decrease in avidity (divalent to monovalent binding), neither the introduction of a tag at the C-terminus of the LC, nor sequential introduction of two payloads at the C-termini of the HC and LC significantly altered their binding ability. Taken together, our data shows that we can engineer a hybridoma cell line to produce high titers of a Fab′ fragment bearing two distinct chemoenzymatic

modification sites on the HC and LC, allowing for orthogonal dual site-specific conjugation of different functionalities.

DISCUSSION

In this study, we present for the first time a strategy to generate dual-tagged Fab′ fragments bearing two orthogonal site-specific modification tags (DTFab′), which can readily be utilized for the chemoenzymatic conjugation with two distinct cargos. Extending on our previous work,[24] we demonstrate the successful engineering of a hybridoma secreting mIgG1 antibodies (anti-CD20 WT) to a stable daughter cell line producing Fab′ fragments carrying an eSrt2A-9 (LAETGG) motif on its HC, and an eSrt4S-9 (LPESGG) motif on its κ LC (anti-CD20 DTFab′). This method enables robust biorthogonal engineering of virtually any antibody-secreting hybridoma, to reproducibly produce high yields of modified DTFab′ molecules. The anti-CD20 DTFab′ daughter cell line secreted high titers of the engineered protein (>1.5 mg.mL^{-1}), which could easily be isolated and modified by orthogonal sortase-mediated transpeptidation. Upon incubation of the DTFab′ protein with either sortase mutant eSrt2A-9 or eSrt4S-9 in the presence of the same fluorescent substrate peptide, we detected exclusive fluorescent labeling of the HC or LC, respectively. As expected[25], the presence of two sortase recognition sites (LAETGG and LPESGG) in close proximity did not affect the specificity of eSrt2A-9 and eSrt4S-9 for their respective motifs, thus enabling site-specific conjugation of two distinct payloads at the C-termini of the HC and LC. As a proof-of-concept, we introduced a fluorescent dye on the HC, and a reactive organic azide on the LC by sequential sortagging (DTFab′FITC/N$_3$). MALDI-TOF and (fluorescent) SDS-PAGE analysis confirmed the identity and the purity of the final product. Importantly, we demonstrated that the target binding capacity of such obtained dual-labeled Fab′ fragment is not compromised, as anticipated due to very mild reaction and purification conditions, and the maximized distance between the cargos and the binding site of the Fab′ fragment. ADC generation through site-specific conjugation offers the advantage to obtain highly homogeneous products with a uniform DAR, thus increasing the therapeutic window.[11] Several strategies to introduce drugs site-specifically have been developed,[27] notably via engineered cysteine introduction at the carboxyl-terminus or the Fab′domain,[28] unnatural amino acids, glycans, or short peptide tags specific for certain enzymes.[23] Among these, sortagging offers the advantage of near-quantitative conversion yields, fast reaction times, and high versatility in the payload, since most cargos can easily be functionalized with an amino-terminal polyglycine motif, and thus act as sortase substrate. Our strategy relies on using two orthogonal variants of the sortase A. Because both variants accept the same nucleophilic recognition motif, the most advantageous conjugation site and order of functionalization can easily be optimized for each cargo, without the need to modify the protein or the substrate.

Others have demonstrated efficient generation of ADCs using transiently expressed recombinant antibodies bearing sortase A LPXTG motifs.[29] Our straightforward CRISPR/HDR hybridoma engineering platform offers the advantage of generating continuously-expressing stable cell lines, resulting in an unlimited source of site-specific functionalizable antibody fragments. More recently, several groups have reported disulfide bond reduction and rebridging strategies to modify native proteins.[30−33] While elegant, such strategies could lead to affinity loss following rebridging and influence antibody rigidity and flexibility,[34,35] which has recently been linked to therapeutic efficacy.[36] By targeting the C-termini of both HC and LC, we do not expect that the conjugation strategy applied in our approach will affect structure or flexibility of the antibody fragment, which is supported by the fact the target binding capacity was not compromised.

Others have described strategies to introduce two cargos site-specifically on a single protein by introducing a combination of tags recognized by orthogonal enzymes, self-labeling tags, engineered residues, or inteins.[37−42] All these strategies have their advantages, but share the requirement to know the sequence of the antibody's variable region to accommodate recombinant expression. Our strategy relies on targeting of the antibody's constant domains and is therefore in principle applicable to any hybridoma, without the need to sequence the variable region. This can be achieved by simply adapting the gRNAs in the Cas9 plasmid, and the homology arms in the HDR template, to the constant domain sequence of the isotype and species of choice.

Combination of several chemotherapeutic drugs to limit the probability of tumor resistance[43] is a powerful strategy, but doses and combinations are limiting due to an invariably associated higher toxicity.[44,45] We foresee that harnessing our platform to generate Fab′ molecules, equipped with two highly cytotoxic payloads with distinct mechanisms of action to target tumors, could lead to a better therapeutic outcome, while reducing the toxicity of the combination therapy. In efforts to explore various combinations of drugs, synthetically easily accessible, rapid, and versatile platforms such as the one presented in this work is instrumental. The versatility can additionally be harnessed to introduce other entities in addition to a drug, such as PEG chains to tune the half-life of the conjugates, and fluorophores or radioligands for theranostic purposes.

EXPERIMENTAL PROCEDURES

Cell Lines and General Culture Conditions. Human CD20-expressing BJAB cells and the mIgG1 anti-CD20-producing hybridoma clone (further referred to as anti-CD20 WT) were kept in RPMI1640 medium (11875093, Thermo-Fisher Scientific), 10% heat-inactivated fetal bovine serum (FBS), 2 mM Ultraglutamine-1 (BE17-605E/U1, Lonza), 1 × Antibiotic−Antimycotic (15240062, ThermoFisher Scientific). Media was additionally supplemented with 50 μM 2-mercaptoethanol (2-ME) (M6250, Sigma-Aldrich). Cells were kept at 37 °C in a 5% CO$_2$ humidified incubator, and passaged three times per week. Cells were checked every 5 weeks for mycoplasma status.

CRISPR/Cas9 Plasmids Generation. The genomic sequence of the Ighg1 constant heavy chain and Igkc constant light chain were identified using the Ensembl genome browser (release 98,[46] accession numbers − Ighg1: ENSMUSG0000-0076614, Igkc: ENSMUSG00000076609). gRNA-H.m1 (5′-CTTGGTGCTGCTGGCCGGGT-3′) and gRNA-L.mκ (5′-GGAATGAGTGTTAGAGACAA-3′) were designed using http://crispor.tefor.net/[47] and ordered as single-stranded oligos from Integrated DNA Technologies (IDT) with the appropriate BbsI overhangs for cloning into the plasmid px330-U6-Chimeric_BB-CBh-hSpCas9, which was obtained as a gift from Feng Zhang (Addgene plasmid #42230). Oligos were phosphorylated using a thermocycler with the T4 PNK enzyme (M0201, New England Biolabs) by incubation at 37

°C for 30 min, and annealed by incubation at 95 °C for 5 min, and cooling at a rate of 0.1 °C/s to 25 °C. Annealed oligos of gRNA-H.m1 and gRNA-L.mκ were cloned into the px330 vector at the BbsI site. Synthetic gene fragments containing homologous arms and desired insert for Fab′ fragment generation and tag insertion were synthesized by IDT and cloned into the PCR2.1 TOPO TA vector (K-450001, ThermoFisher Scientific). All gRNA/Cas9 and HDR plasmids were isolated from DH5α competent E. coli and purified with the NucleoBond Xtra Midi Kit (740410.100, Macherey-Nagel) according to the manufacturer's protocol.

Transfection. Nucleofection of the HDR template and CRISPR-Cas9 vectors was performed as described previously.[24] Briefly, hybridoma cells were assessed for viability, centrifuged (90 g, 5 min), resuspended in phosphate buffered saline (PBS)/1% FBS, and centrifuged again (90 g, 5 min). 1×10^6 cells were resuspended in 100 μL of SF medium with 1 μg of HDR template and 1 μg of Cas9 vector, or 2 μg of GFP vector (control) and transferred to cuvettes for nucleofection with the 4D-Nucleofection System (V4XC-2024, Lonza, CQ-104, Program SF). Transfected cells were quickly transferred to a six-well plate in 6 mL of prewarmed complete medium. The following day, the cells were transferred to a 10 cm Petri dish in 10 mL of complete medium supplemented with blasticidin (10 μg.mL^{-1}, ant-bl-05, Invivogen) or puromycin (5 μg.mL^{-1}, ant-pr-5, Invivogen), which were preliminarily titrated on the wild-type hybridoma cells. Antibiotic pressure was sustained until GFP-transfected hybridomas were not viable, and HDR-transfected cells were confluent (typically between day 10 and 14 for blasticidin, and day 4 and 7 for puromycin). Subsequently, antibiotic-resistant cells were clonally expanded by seeding the hybridomas at the concentration of 0.3 cells per well in 100 μL of complete medium in U-bottom 96-well plates (limiting dilution). After 10 days, supernatant from wells with a high cell density was collected for further characterization.

Genomic DNA Isolation. One week after nucleofection with HDR and targeting constructs, a minimum of 1×10^4 cells of the surviving cell population (bulk) were collected for genomic confirmation of HDR insertion. DNA was extracted using the Isolate II Genomic DNA kit (BIO-52067, Bioline), and was resuspended in ultrapurified water. The target region was PCR amplified using forward primers that anneal in the region directly upstream of the 5′HA for each locus, either fwd.m1 (5′-GTGCCGACTTCAATGTGCTT-3′) or fwd.mκ (5′-GTGCTTGTGTTCAGACTCCC-3′), and a reverse primer that anneals with the IRES in the HDR template rv.ires (5′-GGCTTCGGCCAGTAACGTTA-3′). PCR products were visualized on a 1% (w/v) agarose gel containing Nancy-520 dye (01494, Sigma-Aldrich).

Flow Cytometry. Ten days after limiting dilution, 50 μL of supernatant from wells with high cell densities was transferred to wells in a V-bottom 96-well plate containing 5×10^4 hCD20-expressing BJAB cells. After 20 min of incubation at 4 °C, plates were centrifuged (300 g, 2 min), and supernatant was discarded by flicking. Plates were washed twice with PBS/5% FBS and incubated with anti-His-tag (PE, 362603, BioLegend), anti-mIgG1 (PE, 406608, BioLegend), or anti-Myc-tag (A488, 2279, Cell Signaling Technology). To assess the binding capacity of constructs following CRISPR/Cas9 editing, and several steps of transpeptidation and purification, a competitive binding experiment was performed. Briefly, anti-CD20 parental antibody isolated from the untouched cell line supernatant was dialyzed to borate buffer (pH = 8.5) by

ultracentrifugation, and 100 μg was incubated with 6 equiv of NHS-AF647 (APC-005-1, Jena Bioscience, MW = 1274 Da, 10 mM stock in DMSO) for 2 h at RT in less than 40 μL. Excess label was quenched by diluting the reaction to a final volume of 50 μL using [50 mM Tris pH = 8.0], and incubating 15 min at RT. Labeled antibody was used without further purification. 5 $\times 10^4$ BJAB cells per well were seeded in a V-bottom 96-well plate, and incubated in 50 μL with serial dilutions of Fab′, DTFab′, DTFab′FITC/N$_3$, or the unlabeled parental mAb (concentrations ranging from 150 μg.mL^{-1} to 1.83×10^{-2} μg.mL^{-1}, i.e., 3 μM to 3.66×10^{-4} μM for Fab′ fragments, and 1 μM to 1.22×10^{-4} μM for the mAb). After 10 min of incubation at 4 °C, 50 μL of 1 μg.mL^{-1} labeled parental antibody was added to the wells. After 20 min of incubation at 4 °C, the plate was washed twice, and AF647 fluorescence intensity was acquired by flow cytometry on a MACSQuant plate reader (Miltenyi Biotech).

Antibody Purification from Hybridoma Supernatant. Engineered hybridomas selected for antibody production were cultured in CELLine 1000 flasks (7340389, VWR) following the manufacturer's recommendations. Cells were harvested every other week, supernatant collected by centrifugation (90 g, 5 min), and density gradient purification (LymphoprepTM, 07861, Stem Cell Technologies) was performed to remove dead cells before reseeding them. Supernatant was filtered through a 0.2 μm filter, and supplemented with 10 mM imidazole (I2399, Sigma-Aldrich). Supernatant was incubated with 2 mL of prewashed Ni-NTA beads (30210, Qiagen) at 4 °C on a tube roller for 1 h. Ni-NTA beads were transferred to a disposable chromatography column (7321010, Bio-Rad), washed with 5 column volumes (CV) of ice-cold wash buffer [50 mM Tris pH = 8.0, 150 mM NaCl, 20 mM imidazole], and eluted using 2 × 3 mL of ice-cold elution buffer [50 mM Tris pH = 8.0, 150 mM NaCl, 250 mM imidazole]. Buffer exchange to ice-cold PBS or sortase buffer [50 mM Tris pH = 7.5, 150 mM NaCl] was performed via ultracentrifugation at 4 °C with Amicon Ultra-15 centrifugal filter units (UFC901024, Merck-Millipore). Antibodies from WT hybridomas were purified from medium using Protein G GraviTrap columns (28-9852-55, Sigma-Aldrich). Columns were washed with 10 mL of binding buffer [0.02 M sodium phosphate, pH = 7.0], 20 mL of sample per column was added, and washed with 15 mL of binding buffer. Collection tubes were prefilled with 1 mL of neutralizing buffer [1 M Tris-HCl, pH = 9.0], and column was eluted using 3 mL of elution buffer [0.1 M Glycine-HCl, pH = 2.7]. Antibodies were immediately dialyzed to PBS or sortase buffer by ultracentrifugation at 4 °C. Antibody absorbance was measured using a Nanodrop 2000 (ThermoFisher Scientific) and the UV−vis program. If necessary, antibody absorbance was corrected by measuring the absorbance of the free label at 280 nm and λ_{max}, and calculating the correction factor $F = A_{280label}/A_{\lambda maxlabel}$. Antibody absorbance was corrected by $A_{Ab} = A_{280Ab} - (A_{\lambda maxAb} \times F)$, and concentration was calculated by Beer−Lambert's law, using a correction factor of 1.4 (parental mAb) or 1.35 (Fab′ fragment). Protein purity was assessed on a 12% SDS-PAGE using SYPRO Ruby Protein Gel Stain (S12000, Thermo Fisher Scientific).

Sortase Production and Purification. eSrt(2A-9) and eSrt(4S-9) pET29b were a gift from David Liu (Addgene #75145 and #75146, respectively). Sortase mutants were produced in BL21(DE3) E. coli as reported.[48] Briefly, chemically competent BL21(DE3) were transformed by heat shock, and grown overnight at 30 °C in selective media. The

next day, selective media was inoculated at $OD_{600} \sim 0.05$, and bacteria were grown at 37 °C, 220 rpm to an $OD_{600} \sim 0.6$, and induced with 1 mM IPTG (I5502, Sigma-Aldrich) for 16 h at 25 °C. Bacteria were collected by centrifugation, the pellet washed with [50 mM Tris, 150 mM NaCl], and frozen at −20 °C overnight. Pellets were thawed on ice, and resuspended in lysis buffer [50 mM Tris, 150 mM NaCl, 10 mM imidazole (I0250, Sigma-Aldrich), 20 μg.mL^{-1} of protease inhibitor cocktail (4693159001, Roche), 10% (v/v) glycerol]. Suspension was lysed by sonication on ice (3 × 30 s, 25% amplitude), and centrifuged (8600 g, 30 min, 4 °C). Supernatant was collected, and protein was isolated using Ni-NTA beads. After 1 h of incubation at 4 °C, beads were washed with 100 CV of ice-cold wash buffer [50 mM Tris pH = 7.5, 150 mM NaCl, 10 mM imidazole]. Protein was eluted using 2 × 4 CV ice-cold elution buffer [50 mM Tris pH = 7.5, 150 mM NaCl, 500 mM imidazole, 10% (v/v) glycerol], and washed by ultracentrifugation at 4 °C using a 3 kDa filter (UFC900324, Merck-Millipore) to remove imidazole. Protein concentration was measured on Nanodrop 2000 (MW = 17752 Da, $\varepsilon_{280\ nm}$ = 14565 M^{-1} cm^{-1}), and sortase was stored at −80 °C in sortase buffer [50 mM Tris pH = 7.5, 150 mM NaCl] supplemented with 10% (v/v) glycerol. Protein purity was assessed on a 12% SDS-PAGE using SYPRO Ruby Protein Gel Stain (S12000, Thermo Fisher Scientific).

Sortase-Mediated Transpeptidation. To assess sortase-mediated conjugation, small nucleophilic peptides [H-GGG-C-K(FAM)-NH$_2$], [H-GGG-C-K(FITC)-NH$_2$], and [H-GGG-K(N$_3$)-NH$_2$] were constructed via solid-phase peptide synthesis using a Fmoc/tBu approach and Rink amide resin to yield C-terminal amidated peptides. FAM and FITC were coupled to Lys side chain before peptide cleavage and purified on preparative HPLC using linear gradient of acetonitrile. Peptides were cleaved from the resin by treating the peptidyl-resin with a cleavage cocktail of TFA/TIS/H$_2$O (95:2.5:2.5). [H-GGG-C-K(FAM)-NH$_2$], [H-GGG-C-K(FITC)-NH$_2$], and [H-GGG-K(N$_3$)-NH$_2$] purity was determined by analytical HPLC. Antibodies stored in PBS were dialyzed to sortase buffer via ultracentrifugation at 4 °C. For small scale optimization reactions, 2 μg of Fab′ fragment was reacted, while 500 μg to 1 mg was used for large-scale reactions using proportional volumes. eSrt2A-9- and eSrt4S-9-mediated ligations were carried out using 0.75 equiv of sortase and 50 equiv of nucleophile per equivalent of Fab′ fragment (final antibody concentration 20 μM), in sortase buffer supplemented with CaCl$_2$ at 100 mM final concentration. Reactions were carried out at 37 °C for 1 h. Small-scale reactions were stopped by addition of 100 mM EDTA, and the volume corresponding to 250 ng of Fab′ fragment was loaded onto a reducing SDS-PAGE gel for analysis. Large-scale reactions were incubated at 4 °C on a rotating incubator with 100 μL of prewashed Ni-NTA beads. After 30 min, the mixture was transferred to a disposable spin column, and the flow through collected. Beads were washed with 2 × 500 μL of wash buffer [50 mM Tris pH = 8, 150 mM NaCl, 10 mM imidazole], and the resulting flow-throughs were pooled. Resulting volume was purified by fast protein liquid chromatography (NGC Quest, BioRad) on an ENrichTM SEC70 10 × 300 column (7801070, BioRad) in sortase buffer. Proteins were concentrated on a 0.5 mL 10 kDa filter (UFC501024, Merck-Millipore) by ultracentrifugation. Product purity was assessed on a reducing SDS-PAGE and analyzed for fluorescence and protein signals using the SYPRO Ruby Protein Gel Stain (S12000, ThermoFisher)

on a Typhoon Trio+ imager (GE Healthcare). Protein quantities and densitometry analysis was performed using Fiji (NIH). In addition, the m/z of the conjugates was analyzed on Bruker Microflex LRF MALDI-TOF equipment. Samples were analyzed within a concentration range of 0.3−0.5 mg.mL^{-1} in Milli-Q, using 1 μL each of matrix-sample-matrix sown on the MALDI plate. Matrix: Sinapic acid (trans-3,5-dimethoxy-4-hydroxycinnamic acid) from Sigma-Aldrich (MERCK, D7927) at 10 mg.mL^{-1} in H$_2$O/MeCN (1/1) + 0.1% TFA.

■ ASSOCIATED CONTENT

Ⓢ Supporting Information

The Supporting Information is available free of charge at https://pubs.acs.org/doi/10.1021/acs.bioconjchem.0c00673.

> Full-size SDS-PAGE gels, MALDI-TOF spectra and raw flow cytometry data are available in the supplementary figures. DNA and AA CH1 and Cκ sequences used to design the gRNAs, and HDR templates are available in the supplementary tables. (PDF)

■ AUTHOR INFORMATION

Corresponding Author

Martijn Verdoes − *Department of Tumour Immunology, Radboud Institute for Molecular Life Sciences, 6525 GA Nijmegen, The Netherlands; Institute for Chemical Immunology, 6525 GA Nijmegen, Netherlands;* Email: Martijn.Verdoes@radboudumc.nl

Authors

Camille M. Le Gall − *Department of Tumour Immunology, Radboud Institute for Molecular Life Sciences, 6525 GA Nijmegen, The Netherlands; Oncode Institute, 6525 GA Nijmegen, The Netherlands;* ◎ orcid.org/0000-0002-5890-5115

Johan M. S. van der Schoot − *Department of Tumour Immunology, Radboud Institute for Molecular Life Sciences, 6525 GA Nijmegen, The Netherlands; Oncode Institute, 6525 GA Nijmegen, The Netherlands*

Iván Ramos-Tomillero − *Department of Tumour Immunology, Radboud Institute for Molecular Life Sciences, 6525 GA Nijmegen, The Netherlands; Institute for Chemical Immunology, 6525 GA Nijmegen, Netherlands;* ◎ orcid.org/0000-0003-1928-4149

Melek Parlak Khalily − *Department of Synthetic Organic Chemistry, Radboud University, 6525 AJ Nijmegen, The Netherlands*

Floris J. van Dalen − *Department of Tumour Immunology, Radboud Institute for Molecular Life Sciences, 6525 GA Nijmegen, The Netherlands*

Zacharias Wijfjes − *Department of Tumour Immunology, Radboud Institute for Molecular Life Sciences, 6525 GA Nijmegen, The Netherlands; Institute for Chemical Immunology, 6525 GA Nijmegen, Netherlands*

Liyan Smeding − *Department of Tumour Immunology, Radboud Institute for Molecular Life Sciences, 6525 GA Nijmegen, The Netherlands*

Duco van Dalen − *Department of Tumour Immunology, Radboud Institute for Molecular Life Sciences, 6525 GA Nijmegen, The Netherlands*

Anna Cammarata − *Department of Tumour Immunology, Radboud Institute for Molecular Life Sciences, 6525 GA Nijmegen, The Netherlands*

Kimberly M. Bonger − *Institute for Chemical Immunology, 6525 GA Nijmegen, Netherlands; Department of Synthetic Organic Chemistry, Radboud University, 6525 AJ Nijmegen, The Netherlands;* ⊚ orcid.org/0000-0001-9498-2620

Carl G. Figdor − *Department of Tumour Immunology, Radboud Institute for Molecular Life Sciences, 6525 GA Nijmegen, The Netherlands; Oncode Institute, 6525 GA Nijmegen, The Netherlands; Institute for Chemical Immunology, 6525 GA Nijmegen, Netherlands*

Ferenc A. Scheeren − *Department of Medical Oncology, Leiden University Medical Center, 2333 ZA Leiden, The Netherlands*

Complete contact information is available at:
https://pubs.acs.org/10.1021/acs.bioconjchem.0c00673

Author Contributions

J.M.S.v.d.S., M.V., and F.A.S. conceived the project. K.M.B., C.G.F., F.A.S., and M.V. provided guidance and support. C.M.L., J.M.S.v.d.S., and M.V. designed experiments. C.M.L., J.M.S.v.d.S., and I.R.T. performed the experiments. M.P.K., F.J.v.D., Z.W., L.S., D.v.D., and A.C. contributed experimentally. C.M.L., F.A.S., and M.V. wrote the paper with assistance from all authors. All authors reviewed the manuscript.

Notes

The authors declare no competing financial interest.

■ ABBREVIATIONS

AA, amino acid; ADC, antibody−drug conjugate; bp, base pair; CD, cluster of differentiation; CH1−3, constant heavy chain (1 to 3); Cκ, constant light chain kappa; CRISPR-Cas9, clustered regularly interspaced short palindromic repeats-Cas9 system; DAR, drug-to-antibody ratio; DTFab′, dual-tagged Fab′; EDTA, ethylenediaminetetraacetic acid; Fab′, antigen-binding fragment; 6-FAM, 6-carboxyfluorescein; FBS, fetal bovine serum; FITC, fluorescein isothiocyanate; gRNA, guide ribonucleic acid; HC, heavy chain; HDR, homology directed repair; LC, light chain; mAb, monoclonal antibody; MALDI-TOF, matrix assisted laser desorption ionization-time-of-flight; MFI, mean fluorescence intensity; PCR, polymerase chain reaction; PEG, polyethylene glycol; SDS-PAGE, sodium dodecyl sulfate polyacrylamide gel electrophoresis; SPAAC, strain-promoted azide−alkyne cycloaddition; WT, wild type

■ REFERENCES

(1) FDA approves moxetumomab pasudotox-tdfk for hairy cell leukemia. *Food and Drug Administration Website*; https://www.fda.gov/drugs/resources-information-approved-drugs/fda-approves-moxetumomab-pasudotox-tdfk-hairy-cell-leukemia (2018).

(2) FDA approves polatuzumab vedotin-piiq for diffuse large B-cell lymphoma. *Food and Drug Administration Website*; https://www.fda.gov/drugs/resources-information-approved-drugs/fda-approves-polatuzumab-vedotin-piiq-diffuse-large-b-cell-lymphoma (2019).

(3) FDA approves fam-trastuzumab deruxtecan-nxki for unresectable or metastatic HER2-positive breast cancer. *Food and Drug Administration Website*; https://www.fda.gov/drugs/resources-information-approved-drugs/fda-approves-fam-trastuzumab-deruxtecan-nxki-unresectable-or-metastatic-her2-positive-breast-cancer (2019).

(4) FDA approves inotuzumab ozogamicin for relapsed or refractory B-cell precursor ALL. *Food and Drug Administration Website2*; https://www.fda.gov/drugs/resources-information-approved-drugs/fda-approves-inotuzumab-ozogamicin-relapsed-or-refractory-b-cell-precursor-all (2017).

(5) FDA approves brentuximab vedotin for previously untreated sALCL and CD30-expressing PTCL. *Food and Drug Administration Website2*; https://www.fda.gov/drugs/fda-approves-brentuximab-vedotin-previously-untreated-salcl-and-cd30-expressing-ptcl (2018).

(6) FDA Approves Gemtuzumab Ozogamicin for CD33-positive AML. *Food and Drug Administration Website*; https://www.fda.gov/drugs/resources-information-approved-drugs/fda-approves-gemtuzumab-ozogamicin-cd33-positive-aml (2017).

(7) FDA granted accelerated approval to belantamab mafodotin-blmf for multiple myeloma. *Food and Drug Administration Website*; https://www.fda.gov/drugs/drug-approvals-and-databases/fda-granted-accelerated-approval-belantamab-mafodotin-blmf-multiple-myeloma (2020).

(8) FDA grants accelerated approval to sacituzumab govitecan-hziy for metastatic triple negative breast cancer. *Food and Drug Administration Website*; https://www.fda.gov/drugs/drug-approvals-and-databases/fda-grants-accelerated-approval-sacituzumab-govitecan-hziy-metastatic-triple-negative-breast-cancer (2020).

(9) FDA grants accelerated approval to enfortumab vedotin-ejfv for metastatic urothelial cancer. *Food and Drug Administration Website*; https://www.fda.gov/drugs/resources-information-approved-drugs/fda-grants-accelerated-approval-enfortumab-vedotin-ejfv-metastatic-urothelial-cancer (2019).

(10) *National Clinical Trial database*; https://clinicaltrials.gov/ct2/results?cond=&term=antibody-drug+conjugate&cntry=&state=&city=&dist=&Search=Search.

(11) Beck, A., Goetsch, L., Dumontet, C., and Corvaïa, N. (2017) Strategies and challenges for the next generation of antibody-drug conjugates. *Nat. Rev. Drug Discovery 16*, 315−337.

(12) Vankemmelbeke, M., and Durrant, L. (2016) Third-generation antibody drug conjugates for cancer therapy - A balancing act. *Ther. Delivery 7*, 141−144.

(13) Jain, N., Smith, S. W., Ghone, S., and Tomczuk, B. (2015) Current ADC Linker Chemistry. *Pharm. Res. 32*, 3526−3540.

(14) Li, W., Prabakaran, P., Chen, W., Zhu, Z., Feng, Y., and Dimitrov, D. (2016) Antibody Aggregation: Insights from Sequence and Structure. *Antibodies 5*, 19.

(15) Nelson, A. L. (2010) Antibody fragments: Hope and hype. *MAbs 2*, 77−83.

(16) Burton, D. R. (1985) Immunoglobulin G: Functional sites. *Mol. Immunol. 22*, 161−206.

(17) Andrew, S. M., Pimm, M. V., Perkins, A. C., and Baldwin, R. W. (1986) Comparative imaging and biodistribution studies with an anti-CEA monoclonal antibody and its F(ab)2 and Fab fragments in mice with colon carcinoma xenografts. *Eur. J. Nucl. Med. 12*, 168−175.

(18) Covell, D. G., Barbet, J., Holton, O. D., Black, C. D. V., Weinstein, J. N., and Parker, R. J. (1986) Pharmacokinetics of monoclonal immunoglobulin G1 F(ab' ')2, and Fab′ in mice. *Cancer Res. 46*, 3969−3978.

(19) Xenaki, K. T., Oliveira, S., and van Bergen en Henegouwen, P. M. P. (2017) Antibody or antibody fragments: Implications for molecular imaging and targeted therapy of solid tumors. *Front. Immunol. 8* (1287), 1−6.

(20) Hoffmann, R. M., Coumbe, B. G. T., Josephs, D. H., Mele, S., Ilieva, K. M., Cheung, A., Tutt, A. N., Spicer, J. F., Thurston, D. E., Crescioli, S., et al. (2018) Antibody structure and engineering considerations for the design and function of Antibody Drug Conjugates (ADCs). *Oncoimmunology 7*, 1−11.

(21) Frangos, S., and Buscombe, J. R. (2019) Why should we be concerned about a "g"? *Eur. J. Nucl. Med. Mol. Imaging 46*, 519.

(22) Ton-That, H., Liu, G., Mazmanian, S. K., Faull, K. F., and Schneewind, O. (1999) Purification and characterization of sortase, the transpeptidase that cleaves surface proteins of Staphylococcus aureus at the LPXTG motif. *Proc. Natl. Acad. Sci. U. S. A. 96*, 12424−12429.

(23) Dennler, P., Fischer, E., and Schibli, R. (2015) Antibody conjugates: From heterogeneous populations to defined reagents. *Antibodies 4*, 197−224.

(24) van der Schoot, J. M. S., Fennemann, F. L., Valente, M., Dolen, Y., Hagemans, I. M., Becker, A. M. D., Le Gall, C. M., van Dalen, D., Cevirgel, A., van Bruggen, J. A. C., Engelfriet, M., Caval, T., Bentlage, A. E. H., Fransen, M. F., Nederend, M., Leusen, J. H. W., Heck, A. J. R., Vidarsson, G., Figdor, C. G., Verdoes, M., Scheeren, F. A., et al. (2019) Functional diversification of hybridoma produced antibodies by CRISPR/HDR genomic engineering. *Sci. Adv. 5*, No. eaaw1822.

(25) An, C., Chaikof, E. L., Ham, H. O., Liu, D. R., and Dorr, B. M. (2014) Reprogramming the specificity of sortase enzymes. *Proc. Natl. Acad. Sci. U. S. A. 111*, 13343−13348.

(26) Cong, L., Ran, F. A., Cox, D., Lin, S., Barretto, R., Hsu, P. D., Wu, X., Jiang, W., and Marraffini, L. a. (2013) Multiplex Genome Engineering Using CRISPR/Cas Systems. *Science (Washington, DC, U. S.) 339*, 819−823.

(27) Schumacher, D., Hackenberger, C. P. R., Leonhardt, H., and Helma, J. (2016) Current Status: Site-Specific Antibody Drug Conjugates. *J. Clin. Immunol. 36*, 100−107.

(28) Junutula, J. R., Raab, H., Clark, S., Bhakta, S., Leipold, D. D., Weir, S., Chen, Y., Simpson, M., Tsai, S. P., Dennis, M. S., et al. (2008) Site-specific conjugation of a cytotoxic drug to an antibody improves the therapeutic index. *Nat. Biotechnol. 26*, 925−932.

(29) Beerli, R. R., Hell, T., Merkel, A. S., and Grawunder, U. (2015) Sortase enzyme-mediated generation of site-specifically conjugated antibody drug conjugates with high In Vitro and In Vivo potency. *PLoS One 10*, 1−17.

(30) Ruddle, B. T., Fleming, R., Wu, H., Gao, C., and Dimasi, N. (2019) Characterization of Disulfide Bond Rebridged Fab−Drug Conjugates Prepared Using a Dual Maleimide Pyrrolobenzodiazepine Cytotoxic Payload. *ChemMedChem 14*, 1185−1195.

(31) Kuan, S. L., Wang, T., and Weil, T. (2016) Site-Selective Disulfide Modification of Proteins: Expanding Diversity beyond the Proteome. *Chem. - Eur. J. 22*, 17112−17129.

(32) Walsh, S. J., Omarjee, S., Galloway, W. R. J. D., Kwan, T. T. L., Sore, H. F., Parker, J. S., Hyvönen, M., Carroll, J. S., and Spring, D. R. (2019) A general approach for the site-selective modification of native proteins, enabling the generation of stable and functional antibody-drug conjugates. *Chem. Sci. 10*, 694−700.

(33) Coumans, R. G. E., Ariaans, G. J. A., Spijker, H. J., Renart Verkerk, P., Beusker, P. H., Kokke, B. P. A., Schouten, J., Blomenröhr, M., Van Der Lee, M. M. C., Groothuis, P. G., et al. (2020) A Platform for the Generation of Site-Specific Antibody-Drug Conjugates That Allows for Selective Reduction of Engineered Cysteines. *Bioconjugate Chem. 31*, 2136−2146.

(34) Kline, T., Steiner, A. R., Penta, K., Sato, A. K., Hallam, T. J., and Yin, G. (2015) Methods to Make Homogenous Antibody Drug Conjugates. *Pharm. Res. 32*, 3480−3493.

(35) Murphy, K. M., and Weaver, C. (2016) Antigen Recognition by T and B-cell receptors - The Structure of Typical Antibody Molecule. *Janeway's Immunobiology 9th edition*, 141−146.

(36) Liu, X., Zhao, Y., Shi, H., Zhang, Y., Yin, X., Liu, M., Zhang, H., He, Y., Lu, B., Jin, T., et al. (2019) Human immunoglobulin G hinge regulates agonistic anti-CD40 immunostimulatory and antitumour activities through biophysical flexibility. *Nat. Commun. 10*, 10.

(37) Antos, J. M., Chew, G. L., Guimaraes, C. P., Yoder, N. C., Grotenbreg, G. M., Popp, M. W. L., and Ploegh, H. L. (2009) Site-specific N- and C-terminal labeling of a single polypeptide using sortases of different specificity. *J. Am. Chem. Soc. 131*, 10800−10801.

(38) Harmand, T. J., Bousbaine, D., Chan, A., Zhang, X., Liu, D. R., Tam, J. P., and Ploegh, H. L. (2018) One-Pot Dual Labeling of IgG 1 and Preparation of C-to-C Fusion Proteins Through a Combination of Sortase A and Butelase 1. *Bioconjugate Chem. 29*, 3245−3249.

(39) Wollschlaeger, C., Meinhold-Heerlein, I., Cong, X., Bräutigam, K., Di Fiore, S., Zeppernick, F., Klockenbring, T., Stickeler, E., Barth, S., and Hussain, A. F. (2018) Simultaneous and Independent Dual Site-Specific Self-Labeling of Recombinant Antibodies. *Bioconjugate Chem. 29*, 3586−3594.

(40) De Rosa, L., Cortajarena, A. L., Romanelli, A., Regan, L., and D'Andrea, L. D. (2012) Site-specific protein double labeling by expressed protein ligation: Applications to repeat proteins. *Org. Biomol. Chem. 10*, 273−280.

(41) Lee, M. D., Tong, W. Y., Nebl, T., Pearce, L. A., Pham, T. M., Golbaz-Hagh, A., Puttick, S., Rose, S., Adams, T. E., and Williams, C. C. (2019) Dual Site-Specific Labeling of an Antibody Fragment through Sortase A and π-Clamp Conjugation. *Bioconjugate Chem. 30*, 2539−2543.

(42) Thornlow, D. N., Cox, E. C., Walker, J. A., Sorkin, M., Plesset, J. B., Delisa, M. P., and Alabi, C. A. (2019) Dual Site-Specific Antibody Conjugates for Sequential and Orthogonal Cargo Release. *Bioconjugate Chem. 30*, 1702−1710.

(43) Coldman, A. J., and Goldie, J. H. (1986) A Stochastic Model for the Origin and Treatment of Tumors Containing Drug Resistant Cells. *Bull. Math. Biol. 48*, 279−292.

(44) Mokhtari, R. B., Homayouni, T. S., Baluch, N., Morgatskaya, E., Kumar, S., Das, B., and Yeger, H. (2017) Combination therapy in combating cancer. *Oncotarget 8*, 38022−38043.

(45) Albers, A. E., Grabow, R., Qian, X., Jumah, M. D., Hofmann, V. M., Krannich, A., and Pecher, G. (2017) Efficacy and toxicity of docetaxel combination chemotherapy for advanced squamous cell cancer of the head and neck. *Mol. Clin. Oncol. 7*, 151−157.

(46) Zerbino, D. R., Achuthan, P., Akanni, W., Amode, M. R., Barrell, D., Bhai, J., Billis, K., Cummins, C., Gall, A., Girón, C. G., et al. (2018) Ensembl 2018. *Nucleic Acids Res. 46*, D754−D761.

(47) Haeussler, M., Schönig, K., Eckert, H., Eschstruth, A., Mianné, J., Renaud, J. B., Schneider-Maunoury, S., Shkumatava, A., Teboul, L., Kent, J., et al. (2016) Evaluation of off-target and on-target scoring algorithms and integration into the guide RNA selection tool CRISPOR. *Genome Biol. 17*, 1−12.

(48) Guimaraes, C. P., Witte, M. D., Theile, C. S., Bozkurt, G., Kundrat, L., Blom, A. E. M., and Ploegh, H. L. (2013) Site-specific C-terminal and internal loop labeling of proteins using sortase-mediated reactions. *Nat. Protoc. 8*, 1787−1799.